JOURNAL OF AIRCRAFT
Vol. 43, No. 2, March–April 2006

Minimizing Induced Drag with Wing Twist, Computational-Fluid-Dynamics Validation

Warren F. Phillips,* Spencer R. Fugal,† and Robert E. Spall‡
Utah State University, Logan, Utah 84322-4130

A more practical analytical solution for the effects of wing twist on the performance of a finite wing of arbitrary planform has recently been presented. This infinite series solution is based on Prandtl's classical lifting-line theory, and the Fourier coefficients are presented in a form that depends only on wing geometry. Except for the special case of an elliptic planform, this solution shows that, if properly chosen, wing twist can be used to reduce the induced drag for a wing producing finite lift. A relation for the optimum twist distribution on a wing of arbitrary planform was presented. If this optimum twist distribution is used, the new solution predicts that a wing of any planform can be designed for a given lift coefficient to produce induced drag at the same minimum level as an elliptic wing having the same aspect ratio and no twist. In the present paper, results predicted from this new lifting-line solution are compared with results predicted from computational-fluid-dynamics (CFD) solutions. In all cases, the CFD solutions showed that the drag reduction achieved with optimum twist was equal to or greater than that predicted by lifting-line theory.

Nomenclature

A_n	=	coefficients in the infinite series solution to the lifting-line equation
a_n	=	planform contribution to the coefficients in the infinite series solution to the lifting-line equation
b	=	wingspan
b_n	=	twist contribution to the coefficients in the infinite series solution to the lifting-line equation
C_{Di}	=	induced drag coefficient
C_L	=	lift coefficient
$C_{L,\alpha}$	=	wing lift slope
$\tilde{C}_{L,\alpha}$	=	airfoil section lift slope
c	=	wing-section chord length
R_A	=	wing aspect ratio
R_T	=	wing taper ratio
V_∞	=	magnitude of the freestream velocity
z	=	spanwise coordinate
α	=	angle of attack
α_{L0}	=	zero-lift angle of attack
Γ	=	spanwise section circulation distribution
ε_Ω	=	twist effectiveness
θ	=	change of variables for the spanwise coordinate
κ_D	=	planform contribution to the induced drag factor
κ_{DL}	=	lift-twist contribution to the induced drag factor
$\kappa_{D\Omega}$	=	twist contribution to the induced drag factor
κ_L	=	lift slope factor
Ω	=	total twist, geometric plus aerodynamic
ω	=	normalized twist distribution function

Received 13 December 2004; presented as Paper 2005-1034 at the AIAA 43rd Aerospace Sciences Meeting and Exhibit, Reno, NV, 10–13 January 2005; revision received 26 March 2005; accepted for publication 28 March 2005.

*Professor, Mechanical and Aerospace Engineering Department, 4130 Old Main Hill. Member AIAA.
†Graduate Student, Mechanical and Aerospace Engineering Department, 4130 Old Main Hill.
‡Professor, Mechanical and Aerospace Engineering Department, 4130 Old Main Hill.

I. Introduction

A NEW mathematical solution to a well-established theory of lifting wings has suggested technology that could significantly reduce the drag acting on an aircraft in subsonic flight.[1,2] This drag reduction is accomplished through twisting the wing, or some portion of the wing, in a special manner that depends on wing planform and aircraft operating conditions.

Of course, twisting the wing of an aircraft is not new. Only eight years after the first unpowered human flight by Otto Lilienthal in 1891,[3] and more than four years before their first powered flight in 1903, the Wright brothers began experimenting with wing twist as a means of controlling the rolling motion of an aircraft. Many hours of watching birds in flight led Wilbur to conclude[3] that birds "regain their lateral balance, when partly overturned by a gust of wind, by a torsion of the tips of the wings." This was one of the most important discoveries in aviation history.

Less than two decades later, Ludwig Prandtl[4] published the first theory of lifting wings, which allowed us to mathematically analyze and predict the effects of wing twist. In the 1920s, Hermann Glauert[5] discovered from Prandtl's theory that twisting the two sides of a wing in a symmetric manner could affect the drag acting on the wing. However, under some conditions wing twist was found to reduce drag, and for other conditions twist was found to increase drag.

A recently developed analytical solution to Prandtl's theory[1,2] allows us to predict and maintain the proper distribution and amount of wing twist, which is necessary to minimize the induced drag acting on a lifting wing. With modern sensors and flight computers, which are used on most aircraft today, this new mathematical solution could be incorporated in an active feedback control system to provide the capability for adjusting wing twist on the fly. In this manner minimum possible induced drag could be maintained as the environment and operating conditions change. Although this method of minimizing induced drag does introduce complexity that could increase weight and manufacturing cost, it provides a design alternative worth considering.

Classical lifting-line theory, developed by Ludwig Prandtl[4,6] and published in 1918, was the first analytical method to satisfactorily predict the performance of a lifting wing. Moreover, until the development of the digital computer in the early 1960s, it was the only analytical tool available for wing design. Early comparisons between results predicted from lifting-line theory and experimental data showed excellent agreement for wings of aspect ratio greater than 4. Whereas modern computational fluid dynamics (CFD) is applicable to complex viscous flow across a wide range of flight

conditions, including flow separation and transonic flight, lifting-line theory applies only to subsonic flow in the absence of stall. Nevertheless, even with modern CFD, it is difficult to improve on the induced drag predictions derived from lifting-line theory for low Mach numbers. Prandtl's lifting-line theory is still widely used today because it has the significant advantage of yielding closed-form solutions. Such solutions are not only many orders of magnitude faster to evaluate than modern CFD solutions, but they provide greater insight into how wing design parameters affect wing performance. Closed-form solutions are also well suited to the analytical methods used for design optimization and control.

The first closed-form solution to be obtained from lifting-line theory showed that induced drag could be minimized by using an untwisted wing of elliptic planform. Although an untwisted elliptic wing produces minimum possible induced drag, it is more expensive to manufacture than a simple rectangular wing.

A later analytical solution to Prandtl's theory[5] showed that, although an untwisted tapered wing produces more induced drag than an elliptic wing, it produces significantly less induced drag than an untwisted rectangular wing of the same aspect ratio. The solution showed that, for untwisted wings with linear taper, optimum taper occurs when the tip chord is about 35 to 40% of the root chord. This result, which was first published by the famous English aerodynamicist Hermann Glauert[5] in 1926, has sometimes led to the conclusion that a tapered wing with a tip-to-root chord ratio of about 0.4 always produces significantly less induced drag than a rectangular wing of the same planform area and aspect ratio developing the same lift. As a consequence, tapered wings have long been used as a means of reducing induced drag. The results first presented by Glauert[5] can be misleading if one loses sight of the fact that these results apply only to the case of wings with no twist. The choice of an untwisted wing is quite arbitrary and is not the choice that produces minimum induced drag on a lifting wing, except for the special case of an elliptic planform.

A new closed-form solution that includes spanwise variation in wing twist has recently been developed from lifting-line theory.[1,2] This solution shows that the conclusions sometimes reached from the results first published by Glauert[5] are erroneous. It shows that an unswept wing of any planform shape can be designed with proper twist implementation to produce less induced drag than any tapered wing with no twist. In the study reported herein, this new analytical lifting-line solution was validated by comparison with solutions to the Euler equations obtained using CFL3D[7] and was found to be in excellent agreement.

II. Technical Background

To place the current CFD study in context, a brief review of classical lifting-line theory and recent associated developments[1,2] is presented in this section. Classical lifting-line theory can be used to produce an analytical solution for the spanwise variation in section circulation on a finite wing. For a wing with no sweep or dihedral, combining Helmholtz's vortex theorem with the circulation theory of lift produces the fundamental equation that forms the foundation of Prandtl's lifting-line theory:

$$\frac{2\Gamma(z)}{V_\infty c(z)} + \frac{\tilde{C}_{L,\alpha}}{4\pi V_\infty}\int_{\zeta=-b/2}^{b/2} \frac{1}{z-\zeta}\left(\frac{\mathrm{d}\Gamma}{\mathrm{d}z}\right)_{z=\zeta} \mathrm{d}\zeta = \tilde{C}_{L,\alpha}[\alpha(z) - \alpha_{L0}(z)] \tag{1}$$

In Eq. (1) α and α_{L0} are allowed to vary with the spanwise coordinate to account for geometric and aerodynamic twist. For a given wing design, at a given angle of attack and airspeed, the planform shape, airfoil section lift slope, geometric angle of attack, and zero-lift angle of attack are all known functions of spanwise position. The only unknown in Eq. (1) is the section circulation distribution $\Gamma(z)$.

An analytical solution to Prandtl's lifting-line equation can be obtained in terms of a Fourier sine series. From this solution the circulation distribution is given by

$$\Gamma(\theta) = 2bV_\infty \sum_{n=1}^{\infty} A_n \sin(n\theta) \tag{2}$$

where

$$\theta = \cos^{-1}(-2z/b) \tag{3}$$

and the Fourier coefficients A_n must satisfy the relation

$$\sum_{n=1}^{\infty} A_n \left[\frac{4b}{\tilde{C}_{L,\alpha}c(\theta)} + \frac{n}{\sin(\theta)}\right]\sin(n\theta) = \alpha(\theta) - \alpha_{L0}(\theta) \tag{4}$$

From this circulation distribution, the resulting lift and induced drag coefficients for the finite wing are found to be

$$C_L = \pi R_A A_1 \tag{5}$$

$$C_{\mathrm{Di}} = \pi R_A \sum_{n=1}^{\infty} n A_n^2 \tag{6}$$

The general lifting-line solution expressed in Eqs. (2–6) is not particularly useful for evaluating traditional wing properties because the Fourier coefficients depend on angle of attack and must be reevaluated for each operating point studied.

For a wing with no geometric or aerodynamic twist, α and α_{L0} are independent of θ, and the Fourier coefficients in Eq. (4) can be written as

$$A_n \equiv a_n(\alpha - \alpha_{L0}) \tag{7}$$

which reduces Eq. (4) to

$$\sum_{n=1}^{\infty} a_n \left[\frac{4b}{\tilde{C}_{L,\alpha}c(\theta)} + \frac{n}{\sin(\theta)}\right]\sin(n\theta) = 1 \tag{8}$$

The Fourier coefficients obtained from Eq. (8) depend only on the airfoil section lift slope and wing planform. They are independent of operating conditions.

Historically, the coefficients in the infinite series have usually been evaluated from collocation methods. Typically, the series is truncated to a finite number of terms, and the coefficients in the finite series are evaluated by requiring Eq. (8) to be satisfied at a number of spanwise locations equal to the number of terms in the series. A very straightforward method was first published by Glauert.[5] The most popular method, based on Gaussian quadrature, was originally developed by Multhopp.[8] Another method, based on Fourier series expansion of wing geometry, was first proposed by Lotz[9] and is described by Karamcheti.[10] These methods give identical results in the limit as the number of terms carried in the infinite series becomes large. Furthermore, as shown by Bertin,[11] the methods converge at about the same rate and give similar accuracy for the same level of truncation. For a more detailed presentation of classical lifting-line theory, see Bertin,[11] Anderson,[12] Katz and Plotkin,[13] Kuethe and Chow,[14] McCormick,[15] or Phillips.[16]

For a wing with geometric and/or aerodynamic twist, the definition given by Eq. (7) cannot be used because the aerodynamic angle of attack $(\alpha - \alpha_{L0})$ is not constant. A more useful form of the solution has recently been presented by Phillips.[1] This form of the solution was obtained by using the change of variables

$$\alpha(\theta) - \alpha_{L0}(\theta) \equiv (\alpha - \alpha_{L0})_{\mathrm{root}} - \Omega\omega(\theta) \tag{9}$$

where Ω is defined to be the maximum total twist, geometric plus aerodynamic,

$$\Omega \equiv (\alpha - \alpha_{L0})_{\mathrm{root}} - (\alpha - \alpha_{L0})_{\max} \tag{10}$$

and $\omega(\theta)$ is the local twist distribution, normalized with respect to the maximum total twist

$$\omega(\theta) \equiv \frac{\alpha(\theta) - \alpha_{L0}(\theta) - (\alpha - \alpha_{L0})_{\mathrm{root}}}{(\alpha - \alpha_{L0})_{\max} - (\alpha - \alpha_{L0})_{\mathrm{root}}} \tag{11}$$

The normalized twist distribution function $\omega(\theta)$ is independent of angle of attack and always varies from 0.0 at the root to 1.0 at the point of maximum twist.

Using Eq. (9) in Eq. (4) gives

$$\sum_{n=1}^{\infty} A_n \left[\frac{4b}{\tilde{C}_{L,\alpha} c(\theta)} + \frac{n}{\sin(\theta)} \right] \sin(n\theta) = (\alpha - \alpha_{L0})_{\text{root}} - \Omega\omega(\theta) \tag{12}$$

The Fourier coefficients in Eq. (12) can be conveniently written as

$$A_n \equiv a_n(\alpha - \alpha_{L0})_{\text{root}} - b_n\Omega \tag{13}$$

where

$$\sum_{n=1}^{\infty} a_n \left[\frac{4b}{\tilde{C}_{L,\alpha} c(\theta)} + \frac{n}{\sin(\theta)} \right] \sin(n\theta) = 1 \tag{14}$$

$$\sum_{n=1}^{\infty} b_n \left[\frac{4b}{\tilde{C}_{L,\alpha} c(\theta)} + \frac{n}{\sin(\theta)} \right] \sin(n\theta) = \omega(\theta) \tag{15}$$

Comparing Eq. (14) with Eq. (8), we see that the Fourier coefficients in Eq. (14) are those corresponding to the solution for a wing of the same planform shape but without twist. The solution to Eq. (15) can be obtained in a similar manner and is also independent of angle of attack.

Using Eq. (13) in Eq. (5), the lift coefficient for a wing with twist can be expressed as

$$C_L = \pi R_A A_1 = \pi R_A [a_1(\alpha - \alpha_{L0})_{\text{root}} - b_1\Omega] \tag{16}$$

Using Eqs. (13) and (16) in Eq. (6), the induced drag coefficient is given by

$$C_{\text{Di}} = \frac{C_L^2}{\pi R_A} + \pi R_A \sum_{n=2}^{\infty} n \left[a_n^2 (\alpha - \alpha_{L0})_{\text{root}}^2 - 2a_n b_n (\alpha - \alpha_{L0})_{\text{root}} \Omega + b_n^2 \Omega^2 \right] \tag{17}$$

Equations (16) and (17) can be algebraically rearranged to yield

$$C_L = C_{L,\alpha}[(\alpha - \alpha_{L0})_{\text{root}} - \varepsilon_\Omega \Omega] \tag{18}$$

$$C_{\text{Di}} = \frac{C_L^2(1 + \kappa_D) - \kappa_{\text{DL}} C_L C_{L,\alpha} \Omega + \kappa_{D\Omega} (C_{L,\alpha}\Omega)^2}{\pi R_A} \tag{19}$$

where

$$C_{L,\alpha} = \pi R_A a_1 = \frac{\tilde{C}_{L,\alpha}}{[1 + \tilde{C}_{L,\alpha}/(\pi R_A)](1 + \kappa_L)} \tag{20}$$

$$\kappa_L \equiv \frac{1 - (1 + \pi R_A/\tilde{C}_{L,\alpha}) a_1}{(1 + \pi R_A/\tilde{C}_{L,\alpha}) a_1} \tag{21}$$

$$\varepsilon_\Omega \equiv \frac{b_1}{a_1} \tag{22}$$

$$\kappa_D \equiv \sum_{n=2}^{\infty} n \frac{a_n^2}{a_1^2} \tag{23}$$

$$\kappa_{\text{DL}} \equiv 2\frac{b_1}{a_1} \sum_{n=2}^{\infty} n \frac{a_n}{a_1} \left(\frac{b_n}{b_1} - \frac{a_n}{a_1} \right) \tag{24}$$

$$\kappa_{D\Omega} \equiv \left(\frac{b_1}{a_1} \right)^2 \sum_{n=2}^{\infty} n \left(\frac{b_n}{b_1} - \frac{a_n}{a_1} \right)^2 \tag{25}$$

From Eqs. (18–25), we see that washout increases the zero-lift angle of attack for any wing, but the lift slope for a wing of arbitrary planform shape is not affected by wing twist. Notice that the induced drag for a wing with twist is not zero at zero lift. In addition to the usual component of induced drag, which is proportional to the lift coefficient squared, a wing with twist produces a component of induced drag that is proportional to the twist squared, and this results in induced drag at zero lift. There is also a component of induced drag that varies with the product of the lift coefficient and the twist.

Lifting-line theory predicts that an elliptic wing with no geometric or aerodynamic twist provides a wing geometry that produces minimum possible induced drag for a given lift coefficient and aspect ratio. The chord of an elliptic wing varies with the spanwise coordinate according to the relation

$$c(z) = (4b/\pi R_A)\sqrt{1 - (2z/b)^2}$$

$$\text{or} \qquad c(\theta) = (4b/\pi R_A)\sin(\theta) \tag{26}$$

Using Eq. (26) in Eqs. (14) and (15) yields

$$\sum_{n=1}^{\infty} a_n \left(\frac{\pi R_A}{\tilde{C}_{L,\alpha}} + n \right) \sin(n\theta) = \sin(\theta) \tag{27}$$

$$\sum_{n=1}^{\infty} b_n \left(\frac{\pi R_A}{\tilde{C}_{L,\alpha}} + n \right) \sin(n\theta) = \omega(\theta)\sin(\theta) \tag{28}$$

The well-known solution to Eq. (27) is

$$a_1 = \tilde{C}_{L,\alpha}/(\pi R_A + \tilde{C}_{L,\alpha}), \qquad a_n = 0, \qquad n \neq 1 \tag{29}$$

and the solution to Eq. (28) is given by the Fourier integral

$$b_n = \frac{2}{\pi} \left(\frac{\tilde{C}_{L,\alpha}}{\pi R_A + n\tilde{C}_{L,\alpha}} \right) \int_0^{\pi} \omega(\theta)\sin(\theta)\,\sin(n\theta)\,\mathrm{d}\theta \tag{30}$$

Although elliptic wings with no geometric or aerodynamic twist produce minimum possible induced drag, they are more expensive to manufacture than simple rectangular wings. The tapered wing has commonly been used as a compromise. A tapered wing has a chord that varies linearly with the spanwise coordinate according to the relation,

$$c(z) = \frac{2b}{R_A(1 + R_T)} \left[1 - (1 - R_T) \left| \frac{2z}{b} \right| \right]$$

$$\text{or} \qquad c(\theta) = \frac{2b}{R_A(1 + R_T)} [1 - (1 - R_T)|\cos(\theta)|] \tag{31}$$

Using Eq. (31) in Eqs. (14) and (15) yields the results for a tapered wing,

$$\sum_{n=1}^{\infty} a_n \left\{ \frac{2R_A(1 + R_T)}{\tilde{C}_{L,\alpha}[1 - (1 - R_T)|\cos(\theta)|]} + \frac{n}{\sin(\theta)} \right\} \sin(n\theta) = 1 \tag{32}$$

$$\sum_{n=1}^{\infty} b_n \left\{ \frac{2R_A(1 + R_T)}{\tilde{C}_{L,\alpha}[1 - (1 - R_T)|\cos(\theta)|]} + \frac{n}{\sin(\theta)} \right\} \sin(n\theta) = \omega(\theta) \tag{33}$$

The solution obtained from Eq. (32) for the Fourier coefficients a_n is commonly used for predicting the induced drag for an untwisted tapered wing. This solution is discussed in most engineering textbooks on aerodynamics.[11–16] Figure 1 shows how the induced drag factor from Eq. (23) varies with aspect ratio and taper ratio for tapered wings having no twist and an airfoil section lift slope of 2π. Such results were first published by Glauert[5] and have led to the widely accepted conclusion that a tapered wing with a taper ratio of about 0.4 always produces significantly less induced drag than a rectangular wing of the same aspect ratio developing the same lift coefficient. As a result, tapered wings are commonly used as a means of reducing induced drag.

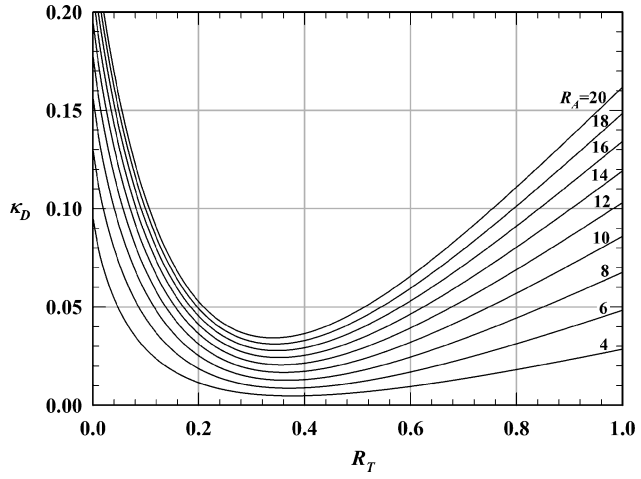

Fig. 1 Planform contribution to induced drag factor for tapered wings.

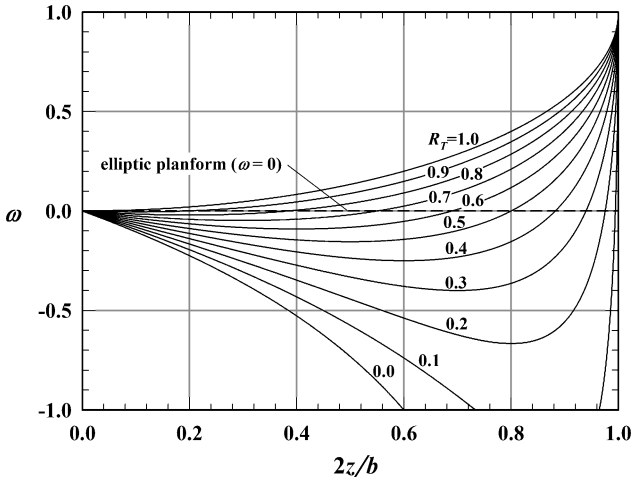

Fig. 2 Optimum twist distribution for wings with linear taper.

When interpreting the results shown in Fig. 1, it has proven easy to lose sight of the fact that these results can be used to predict induced drag only for the special case of wings with no geometric or aerodynamic twist. This is only one of many possible twist distributions that could be used for a wing of any given planform. Furthermore, it is not the twist distribution that produces minimum induced drag with finite lift, except for the special case of an elliptic wing. When the effects of twist are included, it can be shown that the conclusions commonly reached from consideration of only those results shown in Fig. 1 are erroneous.

The induced drag coefficient for a wing with twist can be predicted from Eq. (19) with the definitions given in Eqs. (23–25). For tapered wings with twist, the Fourier coefficients b_n can be obtained from Eq. (33) in exactly the same manner as the coefficients a_n are obtained from Eq. (32). Notice from Eq. (25) that $\kappa_{D\Omega}$ is always positive. Thus, the third term in the numerator on the right-hand side of Eq. (19) always contributes to an increase in induced drag. However, the second term in the numerator on the right-hand side of Eq. (19) can either increase or decrease the induced drag, depending on the signs of κ_{DL} and Ω.

For a wing of any given planform and twist distribution function, the induced drag can be minimized with twist as a result of the tradeoff between the second and third terms in the numerator on the right-hand side of Eq. (19). Thus, Eq. (19) can be used to determine the optimum value of total twist, which will result in minimum induced drag for any given wing planform $c(z)$, twist distribution $\omega(z)$, and lift coefficient C_L. Differentiating Eq. (19) with respect to total twist at constant lift coefficient and setting the result to zero gives the optimum total twist,

$$\Omega_{\mathrm{opt}} = (\kappa_{\mathrm{DL}}/2\kappa_{D\Omega}C_{L,\alpha})C_L \tag{34}$$

Because κ_{DL} is zero for an elliptic wing Eq. (34) shows that an elliptic wing produces minimum induced drag with no twist. For any other planform, an untwisted wing is optimum only at zero lift. Using the value of optimum twist from Eq. (34) in the expression for induced drag coefficient that is given by Eq. (19), we find that the induced drag coefficient for a wing of arbitrary planform with any twist distribution and optimum total twist is given by

$$(C_{\mathrm{Di}})_{\mathrm{opt}} = \left(C_L^2/\pi R_A\right)\left(1 + \kappa_D - \kappa_{\mathrm{DL}}^2/4\kappa_{D\Omega}\right) \tag{35}$$

Because Eq. (25) results in values for $\kappa_{D\Omega}$ that are never negative, we see from Eq. (35) that a wing with optimum twist, as defined by Eq. (34), always produces less induced drag than an untwisted wing of the same planform and aspect ratio operating at the same lift coefficient, unless κ_{DL} is zero.

Lifting-line theory predicts that using the optimum total twist specified by Eq. (34) will result in minimum induced drag for any given wing planform $c(z)$ and twist distribution $\omega(z)$. However, to attain an absolute minimum in induced drag, the spanwise twist distribution must be specified according to the relation presented by Phillips[1]:

$$\omega(z) = 1 - \frac{\sqrt{1-(2z/b)^2}}{c(z)/c_{\mathrm{root}}} \tag{36}$$

With this spanwise variation in wing twist and the optimum total twist specified by Eq. (34), lifting-line theory predicts that an unswept wing of any planform produces the same minimum induced drag as an unswept elliptic wing having the same aspect ratio and operating at the same lift coefficient. For wings with linear taper, this gives

$$\omega(z) = 1 - \frac{\sqrt{1-(2z/b)^2}}{1-(1-R_T)|2z/b|} \tag{37}$$

This twist distribution is shown in Fig. 2 for several values of taper ratio.

For unswept wings with linear taper and the twist distribution specified by Eq. (37), the coefficients defined by Eqs. (24) and (25) can be related to the planform coefficient defined by Eq. (23) (Ref. 2),

$$\kappa_{\mathrm{DL}} = \frac{\pi\tilde{C}_{L,\alpha}}{(1+R_T)C_{L,\alpha}}\kappa_D \tag{38}$$

$$\kappa_{D\Omega} = \left[\frac{\pi\tilde{C}_{L,\alpha}}{2(1+R_T)C_{L,\alpha}}\right]^2\kappa_D \tag{39}$$

Results obtained for wings with linear taper, a section lift slope of 2π, and the twist distribution specified by Eq. (37) are presented in Figs. 3 and 4. After using Eqs. (38) and (39) in Eq. (19), the induced drag for a wing with linear taper and the corresponding optimum twist distribution can be written as

$$C_{\mathrm{Di}} = C_L^2/\pi R_A + (\kappa_D/\pi R_A)[C_L - \pi\tilde{C}_{L,\alpha}\Omega/2(1+R_T)]^2 \tag{40}$$

From Eq. (40), we see that any wing with linear taper and the optimum twist distribution specified by Eq. (37) produces the same minimum induced drag as an elliptic wing with no twist, provided that the total twist is related to the lift coefficient according to

$$\Omega_{\mathrm{opt}} = [2(1+R_T)/\pi\tilde{C}_{L,\alpha}]C_L \tag{41}$$

Because the total twist required to minimize induced drag is proportional to the lift coefficient, it varies with airspeed, altitude, gross weight, and load factor. If only fixed twist is implemented, the wing can only be optimized for a single design operating point. However, with modern sensors and flight computers, which are used on most aircraft today, this new solution could be incorporated in an active feedback control system to adjust wing twist on the fly. In this manner minimum possible induced drag could be maintained as operating conditions change.

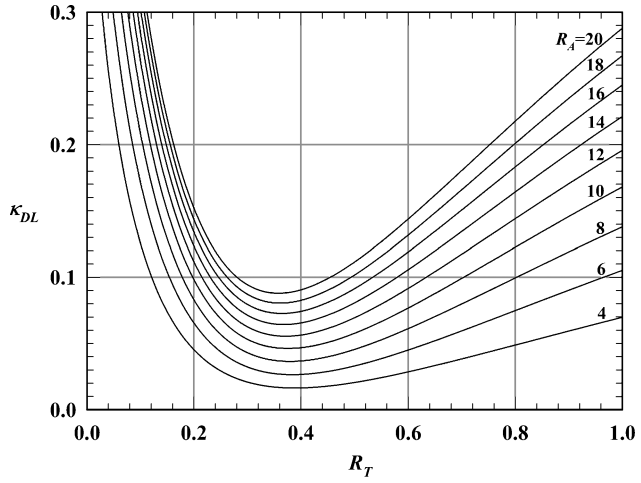

Fig. 3 Lift-twist contribution to the induced drag factor for wings with linear taper and optimum twist distribution.

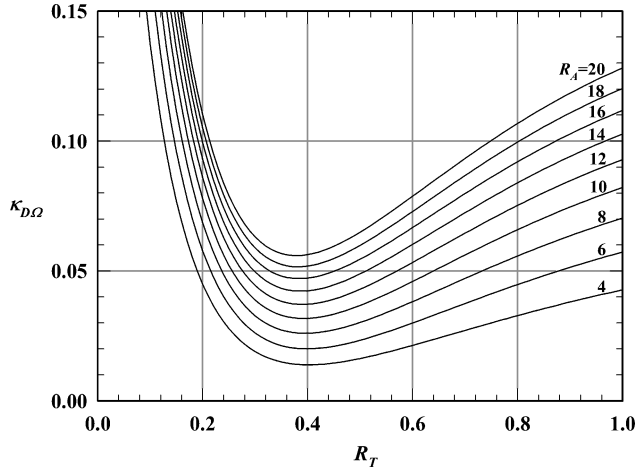

Fig. 4 Twist contribution to the induced drag factor for wings with linear taper and optimum twist distribution.

III. CFD Validation

In this section, induced drag predictions from Eq. (40) are compared with predictions obtained from inviscid CFD computations. Results are presented for three unswept wings; a rectangular wing of aspect ratio 10, a rectangular wing of aspect ratio 20, and a tapered wing of taper ratio 0.4 with an aspect ratio of 20. For each of these three wings, the twist distribution specified by Eq. (37) and plotted in Fig. 2 was used with the optimum total twist specified by Eq. (41). Results obtained for these twist-optimized wings are compared with results obtained for untwisted wings of the same planform and aspect ratio, over a wide range of lift coefficient.

The calculations were performed using version 6 of the computational fluid dynamics code CFL3D.[7] In its most general form, CFL3D is a structured-grid, multizone code that solves the three-dimensional, time-dependent, Reynolds-averaged Navier–Stokes equations using an upwind finite-volume formulation. However, for the calculations presented herein, a steady inviscid formulation was employed to be consistent with the potential flow equations that form the foundation of lifting-line theory. The code uses a third-order upwind-biased interpolation scheme for the convective and pressure terms, and the flux-difference-splitting method of Roe[17] is used to obtain inviscid fluxes at cell faces. Local time stepping, mesh sequencing, and low-Mach-number preconditioning were also used. All computations were performed using C-O grids generated about one semispan of a finite wing. Inflow/outflow boundary conditions were specified on the far-field planes, and symmetry conditions were used along the bounding plane at the wing root. Slip conditions were specified on the wing surface. All results were obtained for a freestream Mach number of 0.044. This low Mach number was chosen to ensure incompressible flow, which is also consistent with the potential-flow foundation of lifting-line theory. The zero-Mach-number solution is directly applicable to Mach numbers as high as 0.3 and with proper compressibility correction can be applied to higher subsonic Mach numbers.

A. Grid Generation

For the present study, grid-generation software was developed to produce C-O grids about one semispan of an unswept tapered wing having either geometric or aerodynamic twist as specified by the user. The software also allows the user to specify the wing aspect ratio, taper ratio, design lift coefficient, and root airfoil cross section. For the present work, nodes were clustered in the chordwise direction near the leading and trailing edges and in the spanwise direction near the wing tip. Nodes were also clustered in the wake region aft of the wing tip, to provide improved resolution of the wing-tip vortex. Figures 5–7 show several sections of a typical grid utilized in the present study.

To keep the wing-tip vortex confined to the wake region where nodes were clustered aft of the wing tip, several different grids were generated for each of the wings studied. As the target lift coefficient was increased, the zero-lift line for the wing was rotated relative to the grid so that the freestream velocity at the target lift coefficient was closely aligned with the x axis of the grid and the region of wake clustering.

B. Grid Resolution

For each wing and operating condition considered, mesh sequencing was employed in the solution procedure using coarse, intermediate, and fine grids, which contained approximately 72,000, 580,000 and 4,600,000 nodes, respectively. The nodes were distributed over a computational domain that extended 10 chord lengths from the wing in all directions. The fine grid was developed using grid-generation software designed specifically to construct C-O grids, which was mentioned in Sec. III.A. The intermediate level grid was derived within CFL3D from the fine grid by deleting alternate points in each direction. The coarse grid was derived from the intermediate grid in a similar manner.

Using converged results from the coarse, intermediate, and fine grids, an improved estimate for the grid-resolved solution was then obtained using the Richardson extrapolation.[18,19] To implement the extrapolation, the procedure described in the August 2004

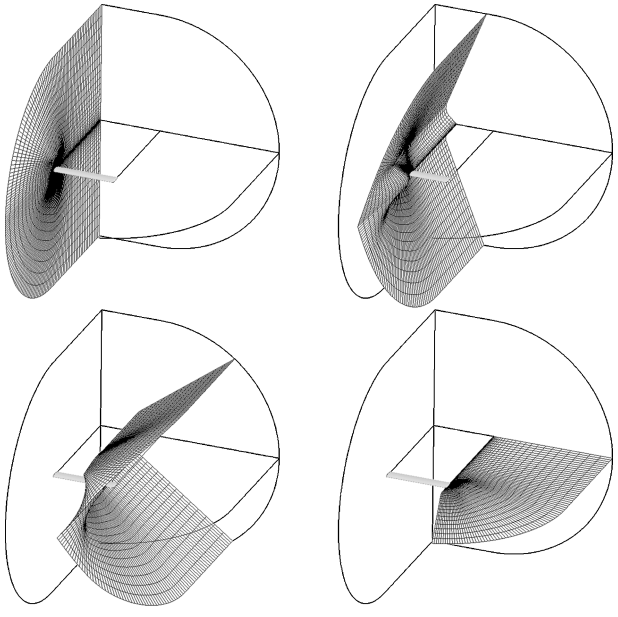

Fig. 5 Constant-k planes for a typical C-O grid.

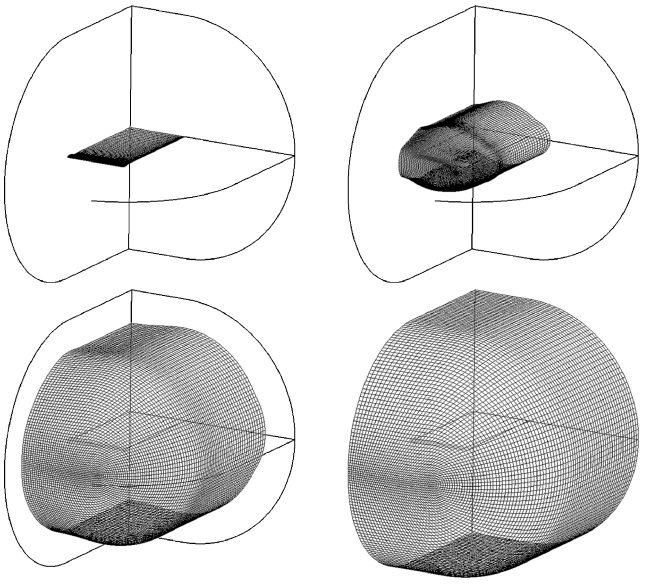

Fig. 6 Constant-j planes for a typical C-O grid.

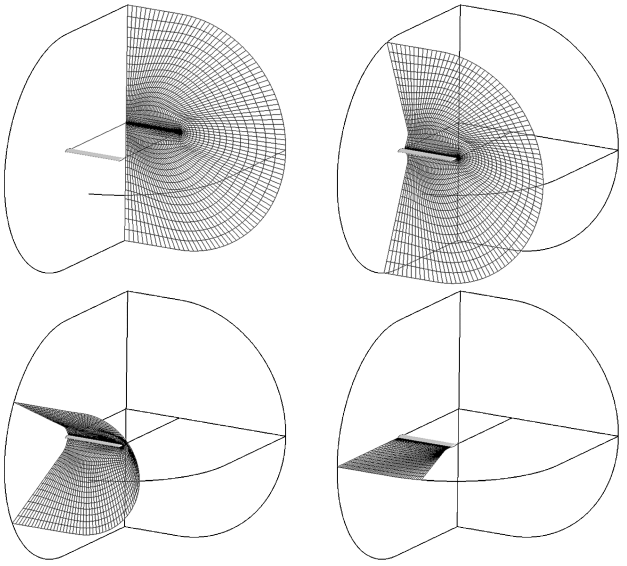

Fig. 7 Constant-i planes for a typical C-O grid.

Journal of Fluids Engineering, "Statement on the Control of Numerical Accuracy," was applied (http://www.asme.org/pubs/journals/fluideng/JFENumAccuracy.pdf). For the sake of completeness, this procedure is outlined in the following paragraph.

First, an average cell size h was computed as

$$h = \left[\frac{1}{N}\sum_{i=1}^{N}\Delta V_i\right]^{\frac{1}{3}}$$

where N is the number of cells and ΔV_i is the volume of the ith cell. If h_1, h_2, and h_3 represent an average cell size on the fine, intermediate, and coarse grids, respectively, then cell size ratios can be defined as $r_{21} = h_2/h_1$ and $r_{32} = h_3/h_2$. For the results presented herein, $r_{21} = r_{32} = 2$. The extrapolated lift coefficient, for instance, is then determined from

$$C_L = \frac{r_{21}^p C_{L1} - C_{L2}}{r_{21}^p - 1}$$

The apparent order of convergence p is determined from

$$p = \frac{|\ell_n|(C_{L3} - C_{L2})/(C_{L2} - C_{L1})| + q(p)|}{\ell_n(r_{21})}$$

where C_{L1}, C_{L2}, and C_{L3} represent the fine, intermediate, and coarse grid solutions, respectively,

$$q(p) = \ell_n\left(\frac{r_{21}^p - s}{r_{32}^p - s}\right) \qquad \text{and} \qquad s = \text{sign}\left(\frac{C_{L3} - C_{L2}}{C_{L2} - C_{L1}}\right)$$

This system was solved for p using fixed-point iteration and gave a typical convergence order of $p \sim 2.5$.

All of the CFD results were plotted in terms of what is commonly referred to as the span efficiency factor for the wing,

$$\text{Span Efficiency Factor} \equiv \left[C_L^2/(\pi R_A)\right]/C_{\text{Di}}$$

Because lifting-line theory predicts that the induced drag produced on an untwisted elliptic wing is given by $C_L^2/(\pi R_A)$, this parameter is often described as the ratio of the induced drag produced by an untwisted elliptic wing to that produced by a wing of any other design. However, for the CFD results this parameter represents the ratio of a lifting-line solution to a CFD solution. Because the CFD solutions might not agree exactly with the lifting-line solutions, this classical interpretation of the span efficiency factor should be used with caution.

For a typical wing with optimum twist, Fig. 8 shows how the solutions obtained from the coarse, intermediate, and fine grids, as well as the extrapolated solution, vary with lift coefficient. Also shown on the figure is the lifting-line solution, which is in close agreement with the extrapolated CFD solution over the range of lift coefficients considered. Similar results for an untwisted wing are shown in Fig. 9.

In addition to the grid-convergence analysis just discussed, which was performed on a fixed computational domain extending 10 chord

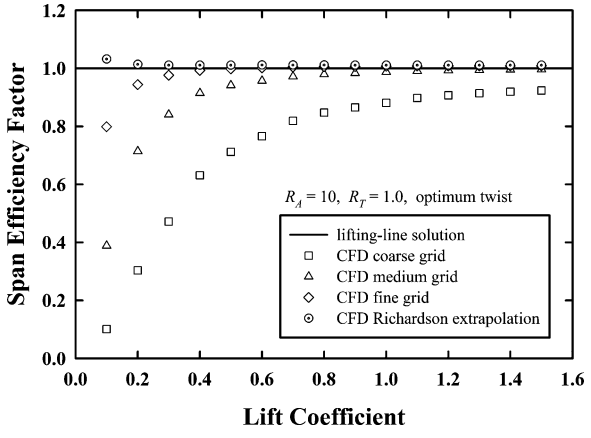

Fig. 8 Grid convergence for a rectangular wing of aspect ratio 10 with optimum twist.

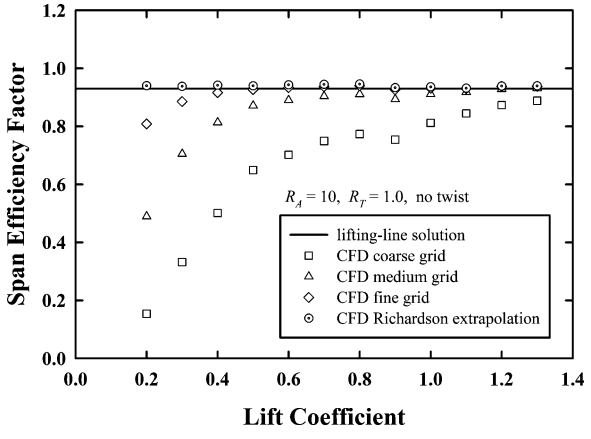

Fig. 9 Grid convergence for a rectangular wing of aspect ratio 10 with no twist.

lengths from the wing in all directions, a larger computational domain was also used for a small subset of the calculations. Results obtained for this larger computational domain, which extended 20 chord lengths from the wing to the outer boundary, revealed a change in the drag coefficient of less than 1% when compared with results obtained from the 10-chord domain. Consequently, the 10-chord domain was deemed sufficient for the remainder of the computations.

C. Results

Figures 10–12 show comparisons between the extrapolated CFD results and those predicted from lifting-line theory, for three wings with and without optimum twist. As already mentioned, these results were obtained from steady inviscid computations at a Mach number of 0.044. In all cases the CFD results predicted that the benefits of employing optimum twist meet or exceed those predicted from lifting-line theory.

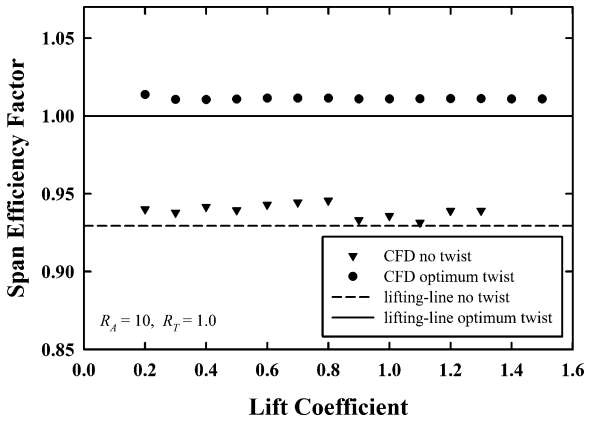

Fig. 10 Lifting-line and CFD results for a rectangular wing of aspect ratio 10.

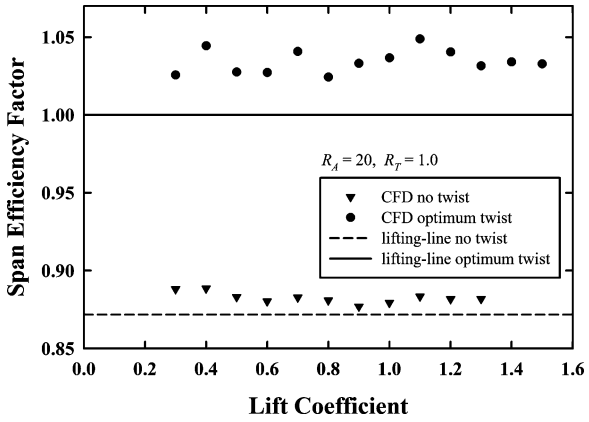

Fig. 11 Lifting-line and CFD results for a rectangular wing of aspect ratio 20.

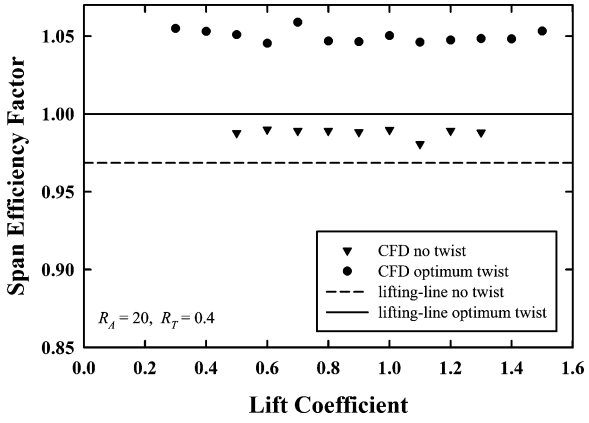

Fig. 12 Lifting-line and CFD results for a tapered wing of aspect ratio 20.

Figure 10 shows the comparison in terms of span efficiency factor for a wing of rectangular planform and aspect ratio 10. Lifting-line theory predicts that an induced drag reduction of approximately 7% can be achieved using optimum twist with this wing planform. This matches the drag reduction observed from the CFD computations almost exactly. For both the untwisted wing and the wing with optimum twist, the extrapolated CFD results showed a slightly lower induced drag than that predicted by lifting-line theory.

Span efficiency results for a more efficient rectangular wing of aspect ratio 20 are shown in Fig. 11. In this case, lifting-line theory predicts nearly a 13% reduction in induced drag for a wing with optimum twist over that for a wing of the same planform with no twist. The extrapolated CFD computations showed a slightly higher induced drag reduction of approximately 15%. Here again, the extrapolated CFD results showed less induced drag than that predicted by lifting-line theory. However, this reduction in induced drag was larger for the wing with optimum twist.

The final comparison examined in the present study is shown in Fig. 12. This tapered wing of aspect ratio 20 and taper ratio 0.4 was the most efficient of the three wings studied. Lifting-line theory predicts that a 3% reduction in induced drag can be achieved by applying optimum twist to an untwisted wing of this planform. The results observed from the extrapolated CFD computations showed a significantly higher induced drag reduction of nearly 6%.

Overall, the CFD results gathered in the present study suggest that lifting-line theory tends to slightly overpredict the induced drag produced by a finite wing. Furthermore, this overprediction seems to be greater for wings with optimum twist than it is for untwisted wings. Thus, the induced drag reduction that is predicted by lifting-line theory for wings with optimum twist would appear to be conservative.

IV. Conclusions

A recently published solution[1,2] to Prandtl's classical lifting-line equation predicts that a wing of any planform shape can be optimized with twist to produce exactly the same minimum induced drag as an elliptic wing with no twist. This solution predicts that minimum possible induced drag for a tapered or rectangular wing occurs when the optimum twist distribution described in Eq. (37) is used together with the optimum total twist specified by Eq. (41). In the present study CFD analysis was used to validate these predictions. The Euler equations were employed to predict the induced drag developed by three wings of different planform over a wide range of lift coefficient. For all three planforms, the induced drag was computed both with and without the optimum twist distribution that is predicted from the new lifting-line solution. Without exception, the CFD results show that the induced drag predictions obtained from lifting-line theory are conservative. In all cases, these CFD results predicted that the induced drag reduction that can be achieved by employing optimum twist is greater than or equal to that predicted from lifting-line theory.

Results presented here show that induced drag can be significantly reduced by proper implementation of wing twist. However, because the amount of twist needed to minimize induced drag varies with lift coefficient, a wing can only be optimized for a single design operating condition when only fixed twist is employed. On the other hand, if variable twist is implemented using an active feedback control system, wing twist could be varied with operating conditions as prescribed by either Eqs. (34) or (41). In this manner minimum induced drag could be maintained as the environment and operating conditions change. This provides a design alternative worth considering.

References

[1]Phillips, W. F., "Lifting-Line Analysis for Twisted Wings and Washout-Optimized Wings," *Journal of Aircraft*, Vol. 41, No. 1, 2004, pp. 128–136.

[2]Phillips, W. F., Alley, N. R., and Goodrich, W. D., "Lifting-Line Analysis of Roll Control and Variable Twist," *Journal of Aircraft*, Vol. 41, No. 5, 2004, pp. 1169–1176.

[3]Anderson, J. D., "The First Aeronautical Engineers," *Introduction to Flight*, 4th ed., McGraw–Hill, New York, 2000, pp. 1–49.

[4]Prandtl, L., "Tragflügel Theorie," *Nachricten von der Gesellschaft der Wissenschaften zu Göttingen*, Ges-chäeftliche Mitteilungen, Klasse, 1918, pp. 451–477.

[5]Glauert, H., "The Monoplane Aerofoil," *The Elements of Aerofoil and Airscrew Theory*, Cambridge Univ. Press, Cambridge, England, U.K., 1926, pp. 137–155.

[6]Prandtl, L., "Applications of Modern Hydrodynamics to Aeronautics," NACA TR-116, June 1921.

[7]Krist, S. L., Biedron, R. T., and Rumsey, C. L., "CFL3D Users Manual (Version 5)," NASA TM-1998-208444, June 1998.

[8]Multhopp, H., "Die Berechnung der Auftriebs Verteilung von Tragflugeln," *Luftfahrtforschung*, Vol. 15, No. 14, 1938, pp. 153–169.

[9]Lotz, I., "Berechnung der Auftriebsverteilung Beliebig Geformter Flugel," *Zeitschrift für Flugtechnik und Motorluftschiffahrt*, Vol. 22, No. 7, 1931, pp. 189–195.

[10]Karamcheti, K., "Elements of Finite Wing Theory," *Ideal-Fluid Aerodynamics*, Wiley, New York, 1966, pp. 535–567.

[11]Bertin, J. J., "Incompressible Flow About Wings of Finite Span," *Aerodynamics for Engineers*, 4th ed., Prentice–Hall, Upper Saddle River, NJ, 2002, pp. 230–302.

[12]Anderson, J. D., "Incompressible Flow over Finite Wings: Prandtl's Classical Lifting-Line Theory," *Fundamentals of Aerodynamics*, 3rd ed., McGraw–Hill, New York, 2001, pp. 360–387.

[13]Katz, J., and Plotkin, A., "Finite Wing: The Lifting-Line Model," *Low-Speed Aerodynamics*, Cambridge Univ. Press, Cambridge, England, U.K., 2001, pp. 167–183.

[14]Kuethe, A. M., and Chow, C. Y., "The Finite Wing," *Foundations of Aerodynamics*, 5th ed., Wiley, New York, 1998, pp. 169–219.

[15]McCormick, B. W., "The Lifting-Line Model," *Aerodynamics, Aeronautics, and Flight Mechanics*, 2nd ed., Wiley, New York, 1995, pp. 112–119.

[16]Phillips, W. F., "Incompressible Flow over Finite Wings," *Mechanics of Flight*, Wiley, New York, 2004, pp. 42–79.

[17]Roe, P. L., "Approximate Reimann Solvers, Parameter Vectors, and Difference Schemes," *Journal of Computational Physics*, Vol. 43, No. 2, 1981, pp. 357–372.

[18]Richardson, L. F., "The Approximate Arithmetical Solution by Finite Differences of Physical Problems Involving Differential Equations, with an Application to the Stresses in a Masonry Dam," *Transactions of the Royal Society of London, A*, Vol. 210, Jan. 1910, pp. 307–357.

[19]Richardson, L. F., and Gaunt, J. A., "The Deferred Approach to the Limit," *Transactions of the Royal Society of London, A*, Vol. 226, Jan. 1927, pp. 299–361.